·临床研究·

蛛网膜下腔出血CT分布对颅内动脉瘤检出的价值

王志平 张义森 曲丽莹

【摘要】 **目的** 通过对比分析不同部位动脉瘤致蛛网膜下腔出血(SAH)的分布差异,探讨其CT分布对提高CTA颅内动脉瘤检出率的价值。**方法** 对2019年1月至2020年10月首都医科大学附属北京天坛医院收治的415例颅内动脉瘤致SAH患者行CT和CTA检查,比较不同部位动脉瘤致SAH的分布差异,对比分析高年资与低年资影像科医师对动脉瘤的检出率。**结果** 共415例患者计463个动脉瘤,包括Ⅰ类动脉瘤324个、Ⅱ类动脉瘤139个;其中责任动脉瘤415个,包括Ⅰ类动脉瘤295个、Ⅱ类动脉瘤120个。Ⅰ类动脉瘤出血主要分布于鞍上池(95.93%,283/295)、环池(90.17%,266/295)、纵裂(86.44%,255/295)、侧裂池(81.02%,239/295)、四叠体池(61.69%,182/295)和桥前池(50.85%,150/295),Ⅱ类动脉瘤出血主要分布于侧裂池(85.83%,103/120)、纵裂(80.83%,97/120)、鞍上池(78.33%,94/120)、环池(77.50%,93/120)、桥前池(67.50%,81/120)和四叠体池(66.67%,80/120);Ⅰ类动脉瘤出血位于鞍上池[95.93%(283/295)对78.33%(94/120);$\chi^2=31.761$,$P=0.001$]和环池[90.17%(266/295)对77.50%(93/120);$\chi^2=11.730$,$P=0.001$]比例高于Ⅱ类动脉瘤,位于桥前池比例低于Ⅱ类动脉瘤[50.85%(150/295)对67.50%(81/120);$\chi^2=9.585$,$P=0.002$)。低年资医师动脉瘤总体检出率(配对χ^2检验:$P=0.000$)和Ⅱ类动脉瘤检出率(配对χ^2检验:$P=0.000$)均低于高年资医师,经培训后Ⅱ类动脉瘤检出率接近高年资医师水平(配对χ^2检验:$P=0.146$)。**结论** 颅内动脉瘤致SAH的CT分布具有规律性,有助于提高CTA颅内动脉瘤检出率。

【关键词】 颅内动脉瘤; 蛛网膜下腔出血; 体层摄影术,螺旋计算机

CT location distribution of subarachnoid hemorrhage and its value in intracranial aneurysm detection

WANG Zhi-ping[1], ZHANG Yi-sen[2], QU Li-ying[1]

[1]Department of Radiology, [2]Department of Interventional Neuroradiology, Beijing Neurosurgical Institute, Beijing Tiantan Hospital, Capital Medical University, Beijing 100070, China

Corresponding author: WANG Zhi-ping (Email: ping1023@139.com)

【**Abstract**】 **Objective** To compare the CT location distribution of subarachnoid hemorrhage (SAH) caused by aneurysms at different locations, and to explore the value of CT hemorrhage distribution for improving the detection of aneurysms in CTA in diagnosing aneurysm. **Methods** Cerebral CT and CTA imaging of 415 patients with aneurysmal SAH from Beijing Tiantan Hospital, Capital Medical University from January 2019 to October 2020 were retrospectively analyzed. The differences of SAH location distribution caused by the aneurysms were compared, and the accuracy of aneurysm diagnosis between junior and senior radiologists were evaluated. **Results** A total of 415 patients had 463 aneurysms, including 324 type-Ⅰ aneurysms and 139 type-Ⅱ aneurysms. There were 415 responsible aneurysms, including 295 type-Ⅰ aneurysms and 120 type-Ⅱ aneurysms. SAH from type-Ⅰ aneurysms was mainly distributed in suprasellar cisterna (95.93%, 283/295), ambient cistern (90.17%, 266/295), longitudinal fissure (86.44%, 255/295), sylvian cistern (81.02%, 239/295), quadrigeminal cistern (61.69%, 182/295) and prepontine cistern (50.85%, 150/295). SAH from type-Ⅱ aneurysms was mainly distributed in sylvian cistern (85.83%, 103/120), longitudinal fissure (80.83%, 97/120), suprasellar cisterna (78.33%, 94/120),

doi:10.3969/j.issn.1672-6731.2022.07.012

基金项目:国家自然科学基金资助项目(项目编号:81801158)

作者单位:100070 首都医科大学附属北京天坛医院放射科(王志平、曲丽莹),神经介入中心 北京神经外科研究所(张义森)

通讯作者:王志平,Email:ping1023@139.com

ambient cistern (77.50%, 93/120), prepontine cistern (67.50%, 81/120) and quadrigeminal cistern (66.67%, 80/120). The proportion of hemorrhage in suprasellar cisterna [95.93% (283/295) vs. 78.33% (94/120); χ^2 = 31.761, P = 0.001] and ambient cistern [90.17% (266/295) vs. 77.50% (93/120); χ^2 = 11.730, P = 0.001] was higher in type-Ⅰ aneurysms than that in type-Ⅱ aneurysms, and the proportion of hemorrhage in prepontine cistern was lower in type-Ⅰ aneurysms than that in type-Ⅱ aneurysms [50.85% (150/295) vs. 67.50% (81/120); χ^2 = 9.585, P = 0.002]. The overall rate of aneurysms detection and type-Ⅱ aneurysms detection in junior radiologists were lower than those in senior radiologists (paired χ^2 test: P = 0.000, 0.000). After the training of SAH distribution, the junior radiologists increased their detection rate of type-Ⅱ aneurysms, and showed no significant difference compared with that of senior radiologists (paired χ^2 test: P = 0.146). **Conclusions** The CT distribution of aneurysmal SAH has regularity. It's important to summarize the characteristics of SAH for improving the detection of aneurysms.

【Key words】 Intracranial aneurysm; Subarachnoid hemorrhage; Tomography, spiral computed
This study was supported by the National Natural Science Foundation of China (No. 81801158).
Conflicts of interest: none declared

蛛网膜下腔出血(SAH)是临床常见的神经科急危重症,病残率和病死率均较高[1]。颅内动脉瘤破裂是引起SAH的最常见原因,占75%~85%[2-3],不同部位动脉瘤引起的SAH分布不同。随着多层CTA的广泛应用,CT联合CTA作为急诊首选检查方法对早期判断SAH病因、准确检出动脉瘤具有重要意义,但对于小型动脉瘤常易漏诊或误诊。本研究通过对比分析不同部位动脉瘤致SAH的分布差异,探讨其CT分布对提高CTA诊断颅内动脉瘤准确性的价值。

资料与方法

一、临床资料

1.纳入与排除标准 (1)经DSA或手术证实SAH系颅内动脉瘤破裂所致。(2)均于发病24 h内行头部CT和CTA检查。(3)年龄<80岁。(4)排除颅脑创伤或脑动静脉畸形等导致的SAH,以及合并中枢神经系统肿瘤或者其他神经系统疾病、严重肝肾功能障碍。

2.一般资料 选择2019年1月至2020年10月首都医科大学附属北京天坛医院急诊收入神经介入中心住院治疗的颅内动脉瘤破裂致SAH患者共415例,男性243例,女性172例;年龄19~79岁,平均(54±16)岁;首发症状为突发性头痛或恶心呕吐占66.02%(274/415),后颈部疼痛占34.46%(143/415),肢体麻木无力占14.94%(62/415),意识障碍占6.75%(28/415)。

二、研究方法

1.头部CT及CTA检查 采用美国GE公司生产的256层螺旋CT扫描仪。(1)CT平扫:平行于听眦线行横断面扫描,管电压120 kV,管电流240 mA,视野(FOV)230 mm×230 mm,矩阵512×512,层厚为5 mm、层间距为零,窗位35 HU、窗宽80 HU,共扫描24层,扫描时间22 s。(2)CTA检查:管电压120 kV,管电流305 mA,层厚0.60 mm、层间距为零;采用高压注射器经肘正中静脉注射碘海醇注射液(规格:350 mgI/ml),注射速度为4~4.50 ml/s,总剂量约为90 ml。绘制颈总动脉时间-密度曲线以获得对比剂峰值时间。获取CT平扫及CTA数据,在系统自带的后处理工作站ADW4.7(美国GE公司)行减影预处理,以及采用标准横断面、冠状位和矢状位最大密度投影(MIP)、曲面重建(CPR)、容积再现(VR)和多平面重建(MPR)等进行图像后处理。

2.图像分析 先由一位低年资影像科医师对CT显示的SAH分布特点进行评估,观察其所累及的脑池情况;再分别由同一位低年资和一位高年资影像科医师对CTA显示的动脉瘤独立阅片,记录其载瘤动脉。

3.动脉瘤检出率 根据诊断"金标准"DSA检查或者术中所见将动脉瘤分为Ⅰ类动脉瘤(即Willis环动脉瘤)和Ⅱ类动脉瘤(即分支动脉瘤),对比分析不同年资医师对动脉瘤的检出率。进一步对低年资医师进行为期2周的SAH分布规律培训,间隔1个月后将图像顺序随机化,再次对Ⅱ类动脉瘤进行评估,并对比分析其与高年资医师对动脉瘤的检出率。

4.统计分析方法 采用SPSS 22.0统计软件进行数据处理与分析。计数资料以相对数构成比(%)

表1 颅内责任动脉瘤部位及SAH累及脑池分布[例(%)]

Table 1. Distribution of intracranial aneurysm and location of SAH [case (%)]

责任动脉瘤部位	个数	鞍上池	环池	侧裂池	纵裂	四叠体池	桥前池	其他
Ⅰ类动脉瘤	295	283(95.93)	266(90.17)	239(81.02)	255(86.44)	182(61.69)	150(50.85)	
ICA	107	102(95.33)	98(91.59)	90(84.11)	87(81.31)	61(57.01)	45(42.06)	
ACoA	123	118(95.93)	105(85.37)	100(81.30)	121(98.37)	71(57.72)	48(39.02)	胼胝体血肿21.14%(26/123)
PCoA	46	44(95.65)	45(97.83)	34(73.91)	31(67.39)	33(71.74)	40(86.96)	
ACA A1	5	5/ 5	4/ 5	4/ 5	5/ 5	3/ 5	3/ 5	
PCA P1	6	6/ 6	6/ 6	5/ 6	5/ 6	6/ 6	6/ 6	
BA	8	8/ 8	8/ 8	6/ 8	6/ 8	8/ 8	8/ 8	第四脑室出血6/8 幕下血肿3/8
Ⅱ类动脉瘤	120	94(78.33)	93(77.50)	103(85.83)	97(80.83)	80(66.67)	81(67.50)	
ACA A2～A4	8	7/ 8	7/ 8	6/ 8	8/ 8	4/ 8	4/ 8	胼胝体血肿7/8
MCA M1	77	69(89.61)	66(85.71)	77(100.00)	71(92.20)	48(62.34)	49(63.64)	颞叶血肿41.56%(32/77)
MCA M2～M4	12	8/12	7/12	12/12	7/12	6/12	6/12	颞叶血肿8/12
PCA P2～P4	7	5/ 7	6/ 7	3/ 7	5/ 7	7/ 7	6/ 7	
VA	10	4/10	5/10	4/10	5/10	10/10	10/10	第四脑室出血9/10 幕下血肿7/10
AICA/PICA	6	1/ 6	2/ 6	1/ 6	1/ 6	5/ 6	6/ 6	第四脑室出血5/6 幕下血肿5/6

ICA, internal carotid artery, 颈内动脉; ACoA, anterior communicating artery, 前交通动脉; PCoA, posterior communicating artery, 后交通动脉; ACA, anterior cerebral artery, 大脑前动脉; PCA, posterior cerebral artery, 大脑后动脉; BA, basilar artery, 基底动脉; MCA, middle cerebral artery, 大脑中动脉; VA, vertebral artery, 椎动脉; AICA, anterior inferior cerebellar artery, 小脑前下动脉; PICA, posterior inferior cerebellar artery, 小脑后下动脉

或率(%)表示,采用配对χ^2检验或Fisher确切概率法。以$P \leqslant 0.05$为差异具有统计学意义。

结　果

本组415例患者计463个颅内动脉瘤,分别为Ⅰ类动脉瘤324个,Ⅱ类动脉瘤139个;其中责任动脉瘤415个,包括Ⅰ类动脉瘤295个,Ⅱ类动脉瘤120个。对比分析责任动脉瘤部位与SAH分布之间关系,由表1可见,Ⅰ类动脉瘤中颈内动脉瘤出血主要分布于鞍上池(95.32%,102/107)、环池(91.59%,98/107),前交通动脉瘤出血主要分布于纵裂(98.37%,121/123)和鞍上池(95.93%,118/123),后交通动脉瘤出血主要分布于环池(97.83%,45/46)和鞍上池(95.65%,44/46),大脑前动脉A1段动脉瘤出血主要分布于鞍上池(5/5)和纵裂(5/5),大脑后动脉P1段动脉瘤和基底动脉瘤出血主要分布于鞍上池(6/6和8/8)、环池(6/6和8/8)、四叠体池(6/6和8/8)以及桥前池(6/6和8/8,图1);Ⅱ类动脉瘤中A2～A4段动脉瘤出血主要分布于纵裂(8/8)、鞍上池(7/8)和环池(7/8),大脑中动脉M1段动脉瘤出血主要分布于侧裂池(100%,77/77)和纵裂(92.21%,71/77),M2～M4段动脉瘤出血主要分布于侧裂池(12/12)和鞍上池(8/12),P2～P4段动脉瘤出血主要分布于四叠体池(7/7)和环池(6/7),椎动脉瘤出血主要分布于四叠体池(10/10)、桥前池(10/10)和第四脑室(9/10),小脑前下动脉瘤/小脑后下动脉瘤出血主要分布于桥前池(6/6)、四叠体池(5/6)和第四脑室(5/6,图2)。Ⅰ类动脉瘤致SAH位于鞍上池[95.93%(283/295)对78.33%(94/120);$\chi^2 = 31.761$, $P = 0.001$]和环池[90.17%(266/295)对77.50%(93/120);$\chi^2 = 11.730$, $P = 0.001$]比例高于Ⅱ类动脉瘤,位于桥前池比例低于Ⅱ类动脉瘤[50.85%(150/295)对67.50%(81/120);$\chi^2 = 9.585$, $P = 0.002$],且差异具有统计学意义。此外,部分动脉瘤致SAH还有其特征性,A2～A4段动脉瘤和前交通动脉瘤均可伴发胼胝体周围血肿,但二者发生率差异有统计学意义[7/8对21.14%(26/123);校正$\chi^2 = 14.209$, $P = 0.000$];M1段和M2～M4段动脉瘤伴发颞叶血肿的概率分别为41.56%(32/77)和8/12,均高于颈内动脉瘤[0(0/107)]且差异有统计学意义(Fisher确切概率法:$P = 0.000$, 0.000);椎动脉瘤和小脑前下动脉瘤/小脑后下动脉瘤伴发幕下血肿的概率分别为7/10和5/6,

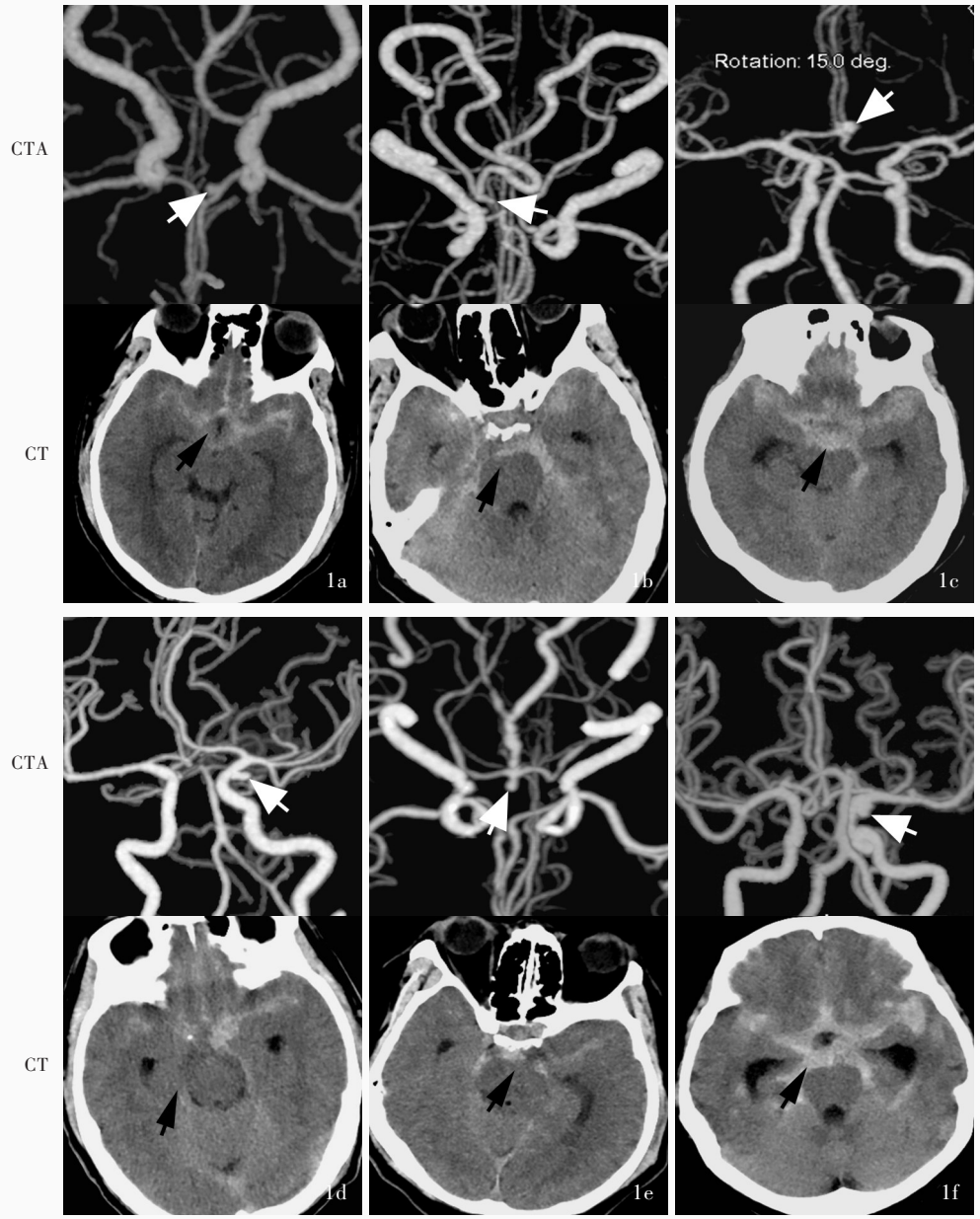

图1　Ⅰ类动脉瘤及所致SAH的CTA三维容积再现及CT平扫所见　1a　左大脑前动脉A1段动脉瘤(粗箭头所示)出血分布于鞍上池、纵裂和侧裂池(细箭头所示)　1b　右大脑后动脉P1段动脉瘤(粗箭头所示)出血分布于桥前池、环池和侧裂池(细箭头所示)　1c　前交通动脉瘤(粗箭头所示)出血分布于鞍上池、环池、纵裂和侧裂池(细箭头所示)　1d　左后交通动脉瘤(粗箭头所示)出血分布于鞍上池、环池和侧裂池(细箭头所示)　1e　基底动脉尖动脉瘤(粗箭头所示)分布于桥前池、环池和鞍上池(细箭头所示)　1f　左颈内动脉交通段动脉瘤(粗箭头所示)出血分布于鞍上池、侧裂池和环池(细箭头所示)

Figure 1　3D volume reconstruction of CTA and CT findings of type-Ⅰ aneurysms and associated SAH　SAH from aneurysm of the left ACA A1 segment (thick arrow indicates) located in suprasellar cistern, longitudinal fissure and sylvian cistern (thin arrow indicates, Panel 1a). SAH from aneurysm of the right PCA P1 segment (thick arrow indicates) located in prepontine cistern, ambinent cisterna and sylvian cistern (thin arrow indicates, Panel 1b). SAH from the aneurysm of ACoA (thick arrow indicates) located in suprasellar cistern, ambinent cisterna, longitudinal fissure and sylvian cistern (thin arrow indicatesm, Panel 1c). SAH from aneurysm of the left PCoA (thick arrow indicates) located in suprasellar cistern, ambinent cisterna and sylvian cistern (thin arrow indicates, Panel 1d). SAH from the BA aneurysm (thick arrow indicates) located in prepontine cistern, ambinent cisterna and suprasellar cistern (thin arrow indicates, Panel 1e). SAH from aneurysm of the left ICA communication segment (thick arrow indicates) located in suprasellar cistern, sylvian cistern and cisterna ambiens (thin arrow indicates, Panel 1f).

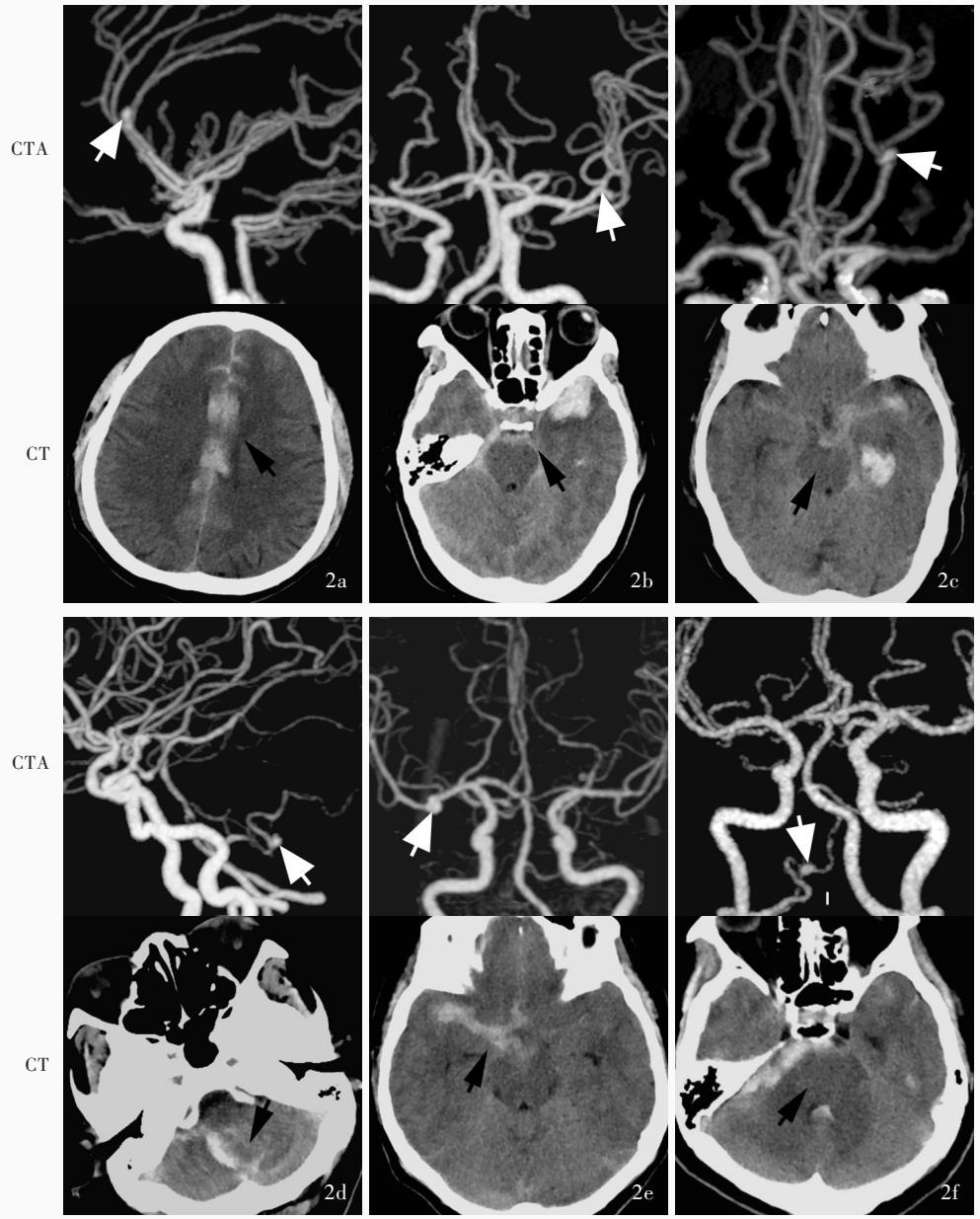

图2 Ⅱ类动脉瘤及其所致SAH的CTA三维容积再现及CT平扫所见 2a 左大脑前动脉A3段动脉瘤(粗箭头所示)出血分布于纵裂,并可见胼胝体周围血肿(细箭头所示) 2b 左大脑中动脉M2段动脉瘤(粗箭头所示)出血分布于环池、侧裂池,并可见左侧颞叶血肿(细箭头所示) 2c 左大脑后动脉P3段动脉瘤(粗箭头所示)出血分布于环池、四叠体池、鞍上池、侧裂池,并可见左侧颞叶内侧血肿(细箭头所示) 2d 右小脑后下动脉瘤(粗箭头所示)出血分布于第四脑室,并可见幕下血肿(细箭头所示) 2e 右大脑中动脉M1段动脉瘤(粗箭头所示)出血分布于侧裂池、鞍上池,并可见纵裂出血(细箭头所示) 2f 右椎动脉瘤(粗箭头所示)出血分布于脑桥小脑角池、第四脑室和桥前池(细箭头所示)

Figure 2 3D volume reconstruction of CTA and CT findings of type-Ⅱ aneurysms and associated SAH SAH from aneurysm of the left ACA A1 segment (thick arrow indicates) located in longitudinal fissure, and pericallosum hematoma existed (thin arrow indicates, Panel 2a). SAH from aneurysm of the left MCA M2 segment (thick arrow indicates) located in ambient cisterna and sylvian cistern, and the left temporal lobe hematoma existed (thin arrow indicates, Panel 2b). SAH from aneurysm of the left PCA P3 segment (thick arrow indicates) located in ambient cisterna, quadrigeminal cistern, suprasellar cistern and sylvian cistern (thin arrow indicates, Panel 2c). SAH from aneurysm of the right PICA (thick arrow indicates) located in the fourth ventricle, and subatentorial hematoma existed (thin arrow indicates, Panel 2d). SAH from aneurysm of the right MCA M1 segment (thick arrow indicates) located in right sylvian cistern, suprasellar cistern and longitudinal fissure (thin arrow indicates, Panel 2e). SAH from aneurysm of the right VA (thick arrow indicates) located in right cerebellopontine angle, the fourth ventricle and prepontine cistern (thin arrow indicates, Panel 2f).

表2 高年资与低年资医师对动脉瘤总体检出率的比较[例(%)]*

Table 2. Comparison of the detection rate of aneurysms between senior and junior radiologists [case (%)]*

低年资医师	高年资医师		
	检出	未检出	合计
检出	402(86.83)	7(1.51)	409(88.34)
未检出	32(6.91)	22(4.75)	54(11.66)
合计	434(93.74)	29(6.26)	463(100.00)

*paired χ^2 test: $P=0.000$,配对χ^2检验:$P=0.000$

表3 高年资与低年资医师对Ⅰ类动脉瘤检出率的比较[例(%)]*

Table 3. Comparison of the detection rate of type-Ⅰ aneurysms between senior and junior radiologists [case (%)]*

低年资医师	高年资医师		
	检出	未检出	合计
检出	292(90.12)	6(1.85)	298(4.94)
未检出	16(4.94)	10(3.09)	26(8.02)
合计	308(95.06)	16(4.94)	324(100.00)

*paired χ^2 test: $P=0.052$,配对χ^2检验:$P=0.052$

表4 高年资与低年资医师对Ⅱ类动脉瘤检出率的比较[例(%)]*

Table 4. Comparison of the detection rate of type-Ⅱ aneurysms between senior and junior radiologists [case (%)]*

低年资医师	高年资医师		
	检出	未检出	合计
检出	110(79.14)	1(0.72)	111(79.86)
未检出	16(11.51)	12(2.59)	28(20.14)
合计	126(90.65)	13(2.81)	139(100.00)

*paired χ^2 test: $P=0.000$,配对χ^2检验:$P=0.000$

表5 高年资与培训后的低年资医师对Ⅱ类动脉瘤检出率的比较[例(%)]*

Table 5. Comparison of the detection rate of type-Ⅱ aneurysms between senior and junior radiologists after training [case (%)]*

培训后的低年资医师	高年资医师		
	检出	未检出	合计
检出	117(84.17)	3(2.16)	120(86.33)
未检出	9(6.47)	10(7.19)	19(13.67)
合计	126(90.65)	13(9.35)	139(100.00)

*paired χ^2 test: $P=0.146$,配对χ^2检验:$P=0.146$

均高于P2~P4段动脉瘤[0(0/7)]且差异有统计学意义(Fisher确切概率法:$P=0.010$,0.005);基底动脉瘤(3/8)、椎动脉瘤(7/10)和小脑前下动脉瘤/小脑后下动脉瘤(5/6)均伴发幕下血肿,但两两比较差异均未达到统计学意义(Fisher确切概率法:$P=0.342$,0.138,1.000)。

本组463个动脉瘤,高年资医师总体检出率为93.74%(434/463),低年资医师为88.34%(409/463),二者差异有统计学意义($P=0.000$);324个Ⅰ类动脉瘤,高年资医师检出率为95.06%(308/324),低年资医师为91.98%(298/324),二者差异无统计学意义($P=0.052$;表2,3);139个Ⅱ类动脉瘤,高年资医师检出率为90.65%(126/139),低年资医师为79.86%(111/139)、经SAH分布规律培训后为86.33%(120/139),低年资医师检出率低于高年资医师($P=0.000$),但经培训后与高年资医师差异无统计学意义($P=0.146$;表4,5)。

讨 论

由于载瘤动脉不同,颅内动脉瘤破裂致SAH和颅内血肿的分布亦有一定的特征性[4-5],首选CT平扫,根据CT显示的SAH分布大致判断出动脉瘤部位,可在无条件进一步行CTA检查的医院初步指导治疗[6-7]。结合CT平扫显示的SAH分布特点以及CTA可以更准确地检出临床易漏诊的微小动脉瘤和Ⅱ类动脉瘤。

本研究分析415例颅内动脉瘤患者计415个责任动脉瘤与SAH分布之间的关系,发现Ⅰ类动脉瘤致SAH主要分布于鞍上池和环池,并根据动脉瘤具体部位,出血累及脑池的顺序略有不同,如颈内动脉瘤出血主要聚集于鞍上池和环池,前交通动脉瘤出血主要聚集于纵裂和鞍上池,后交通动脉瘤出血主要聚集于环池和鞍上池,大脑前动脉A1段动脉瘤出血主要聚集于鞍上池和纵裂,大脑后动脉P1段动脉瘤和基底动脉瘤出血主要聚集于鞍上池、环池、四叠体池和桥前池。部分大脑前动脉瘤、大脑中动脉瘤和大脑后动脉瘤出血可伴发邻近脑叶血肿,尤以Ⅱ类动脉瘤出血更易发生邻近脑叶血肿。尽管既往研究业已证实,SAH分布特点可部分提示动脉瘤部位,对临床明确出血病因和及时评估具有重要作用[8-11],但本研究样本量较大,从而更全面地总结出各部位动脉瘤致SAH的分布规律。

本研究还对比分析高年资与低年资影像科医师对动脉瘤的检出率,结果显示,高年资与低年资

医师对Ⅰ类动脉瘤的检出率相当;但对于非Willis环的Ⅱ类动脉瘤,低年资医师的检出率低于高年资医师,提示此类动脉瘤临床易漏诊。根据CT显示的此类动脉瘤致SAH分布特点,总结出临床易漏诊动脉瘤的特征性表现:A2段及远端Ⅱ类动脉瘤出血主要聚集于纵裂、鞍上池和胼胝体周围,其中胼胝体周围血肿发生率高于Ⅰ类动脉瘤;大脑中动脉瘤出血主要聚集于侧裂池、纵裂、鞍上池和颞叶,其中颞叶血肿发生率高于Ⅰ类动脉瘤;椎动脉瘤或者小脑前下动脉瘤/小脑后下动脉瘤出血主要聚集于桥前池、四叠体池和第四脑室,其中幕下血肿发生率高于P2~P4段动脉瘤。Sawicki等[12]认为,动脉瘤破裂并发颅内血肿时,根据血肿部位判断动脉瘤部位较单纯观察脑池、脑沟受累情况更容易。低年资医师经过为期2周的SAH分布规律培训后,对非Willis环的Ⅱ类动脉瘤的检出率增加,接近高年资医师水平。既往关于颅内血肿与动脉瘤部位关系的研究样本量较小,或仅针对特定部位动脉瘤[13-14],本研究更全面地总结颅内血肿与动脉瘤的对应关系,从而为术前判断提供重要依据。

本研究Ⅱ类动脉瘤样本量相对较小,对于某些出血特点如颅内血肿与动脉瘤的对应关系尚待扩大样本量进一步验证;本研究仅对比分析影像学特点,关于动脉瘤致SAH的预后及其与出血的关系等临床重点关注内容,尚待进一步验证。

综上所述,CT出血分布特点在动脉瘤致SAH的病因诊断中具有重要参考价值,CT平扫结合CTA使颅内动脉瘤的诊断效率和诊断准确性显著提高,今后尚待进一步探讨动脉瘤部位和出血特点对判断临床预后的意义。

利益冲突 无

参 考 文 献

[1] Korja M, Kaprio J. Controversies in epidemiology of intracranial aneurysms and SAH[J]. Nat Rev Neurol, 2016, 12:50-55.

[2] Macdonald RL, Schweizer TA. Spontaneous subarachnoid haemorrhage[J]. Lancet, 2017, 389:655-666.

[3] van Gijn J, Kerr RS, Rinkel GJ. Subarachnoid haemorrhage[J]. Lancet, 2007, 369:306-318.

[4] Korja M, Kivisaari R, Rezai Jahromi B, Lehto H. Size and location of ruptured intracranial aneurysms: consecutive series of 1993 hospital-admitted patients[J]. J Neurosurg, 2017, 127: 748-753.

[5] Karttunen AI, Jartti PH, Ukkola VA, Sajanti J, Haapea M. Value of the quantity and distribution of subarachnoid haemorrhage on CT in the localization of a ruptured cerebral aneurysm[J]. Acta Neurochir (Wien), 2003, 145:655-661.

[6] Gao J, Yu WN, Liu X, Liu Y, Miao L, Wang M, Wang Y, Zhang H. Accuracy of non-enhanced computed tomography in locating ruptured aneurysms in patients with aneurysmal subarachnoid hemorrhage and its predictive value for prognosis [J]. Shi Yong Xin Nao Fei Xue Guan Bing Za Zhi, 2021, 29:97-103.[高洁, 玉王宁, 刘鑫, 刘岩, 苗玲, 王敏, 王莹, 张辉. 非增强CT扫描定位动脉瘤性蛛网膜下腔出血患者破裂动脉瘤的准确性及其对预后的预测价值研究[J]. 实用心脑肺血管病杂志, 2021, 29:97-103.]

[7] Feng YG, Liang CQ, Li HT, Tang WZ, Wang Y, Mou LK. New classification of subarachnoid hemorrhage according to CT image and its clinical value in the patients with ruptured middle cerebral artery aneurysms [J]. Zhongguo Lin Chuang Shen Jing Wai Ke Za Zhi, 2012, 17:470-472.[丰育功, 梁崇乾, 李环廷, 唐万忠, 王毅, 牟立坤. 大脑中动脉动脉瘤破裂致蛛网膜下腔出血的新CT分型及其临床价值(附121例报告)[J]. 中国临床神经外科杂志, 2012, 17:470-472.]

[8] Feng YG, Liu B, Hou XQ, Wang WM. CT application in the clinical diagnosis of aneurysmal subarachnoid hemorrhage[J]. Zhonghua Shen Jing Yi Xue Za Zhi, 2003, 2:343-345.[丰育功, 刘滨, 侯晓群, 王伟民. CT在诊断动脉瘤性蛛网膜下腔出血中的临床应用研究(附140例报道)[J]. 中华神经医学杂志, 2003, 2:343-345.]

[9] Li T, Fan BY, Zhao XC, Wang XR, Wang ZS, Cheng J, Wang JG. CT diagnosis of spontaneous subarachnoid hemorrnage: an analysis of 1000 cases[J]. Zhonghua Fang She Xue Za Zhi, 1999, 33:94-96.[李廷, 范宝瑜, 赵欣春, 王学仁, 王振山, 程杰, 王君贵. 自发性蛛网膜下腔出血1000例的CT诊断[J]. 中华放射学杂志, 1999, 33:94-96.]

[10] Korja M, Lehto H, Juvela S. Lifelong rupture risk of intracranial aneurysms depends on risk factors: a prospective Finnish cohort study[J]. Stroke, 2014, 45:1958-1963.

[11] Li JW, Xiang SS, Ling F, Zhang HQ, Li GL. Subarachnoid hemorrhage caused by vertebrobasilar dolichoectasia complicated with basilar artery dissecting aneurysm: one case report[J]. Zhongguo Xian Dai Shen Jing Ji Bing Za Zhi, 2016, 16:845-849.[李静伟, 向思诗, 凌锋, 张鸿祺, 李桂林. 椎基底动脉延长扩张症伴基底动脉夹层动脉瘤致蛛网膜下隙出血一例[J]. 中国现代神经疾病杂志, 2016, 16:845-849.]

[12] Sawicki M, Kościukiewicz K, Jeżewski D, Chełstowski K, Gołofit P, Skoczylas MM, Gębka M, Grabizna K, Kołaczyk K, Zwarzany Ł, Sagan L, Poncyljusz W. Diagnostic value of non-enhanced computed tomography in identifying location of ruptured cerebral aneurysm in patients with aneurysmal subarachnoid haemorrhage[J]. Neurol Neurochir Pol, 2020, 54: 47-53.

[13] Burkhardt JK, Winkler EA, Lasker GF, Yue JK, Lawton MT. Isolated abducens nerve palsy associated with subarachnoid hemorrhage: a localizing sign of ruptured posterior inferior cerebellar artery aneurysms[J]. J Neurosurg, 2018, 128:1830-1838.

[14] Zuo TS, Xu KX, Wang J. CT distribution law of CT of aneurysmal subarachnoid hemorrhage and comparative analysis of aneurysmal distribution of MSCTA[J]. Zhongguo Yi Yao Ke Xue, 2015, 5:14-18.[左涛生, 许开喜, 王金. 动脉瘤性蛛网膜下腔出血的CT分布规律及MSCTA动脉瘤分布对照分析[J]. 中国医药科学, 2015, 5:14-18.]

(收稿日期:2022-07-14)
(本文编辑:彭一帆)